PREDICTING MENTAL WORKLOAD OF USING EXOSKELETONS FOR CONSTRUCTION WORK: A DEEP LEARNING APPROACH

Adedeji Afolabi, Research Associate
Virginia Polytechnic Institute and State University, Virginia, United States
adedeji@vt.edu

Anthony Yusuf, Ph.D Student
Virginia Polytechnic Institute and State University, Virginia, United States
anthonyy@vt.edu

Abiola Akanmu, Associate Professor
Virginia Polytechnic Institute and State University, Virginia, United States
abiola@vt.edu

SUMMARY: Exoskeletons are gaining attention as a potential solution for addressing back injury in the construction industry. However, using active back-support exoskeletons in construction can trigger unintended consequences which could increase the mental workload of workers. Prolonged increase in mental workload could impact workers' wellbeing and productivity. Predicting mental workload during exoskeleton use could inform strategies to mitigate the triggers. This study investigates two machine-learning frameworks for predicting mental workload using an active back-support exoskeleton for construction work. Laboratory experiments were conducted wherein electroencephalography (EEG) data was collected from participants wearing an active back-support exoskeleton to perform flooring tasks. The EEG data underwent preprocessing, including band filtering, notch filtering, and independent component analysis, to remove artifacts and ensure data quality. A regression-based Long Short-Term Memory (LSTM) network and a hybrid model of convolutional neural network and LSTM were trained to forecast future time steps of the processed EEG data. The performance of the networks was evaluated using root mean square error and r-squared. An average root mean square error of 0.162 and r-squared of 0.939 indicate that the LSTM network has a better predictive power across all the EEG channels. Results of the comparison between the actual and predicted mental workload also show that about 75% of the variance in the actual mental workload is captured in the predicted mental workload. This study enhances understanding of the unintended consequences of using exoskeletons in construction work. The results highlight the effectiveness of various convolutional neural network methods in identifying key EEG data features, offering guidance for algorithm selection in future applications. Additionally, the study identifies the most suitable brain channels for assessing mental workload during exoskeleton use, aiding the development of EEG devices that optimize cost-effectiveness, explanatory power, and minimal channels. This study provides valuable insights for stakeholders to understand the impact of mental workload while using exoskeletons and discovering opportunities for mitigation.

KEYWORDS: Work-related musculoskeletal disorders, Exoskeleton, Mental workload, Electroencephalogram, Long Short-Term Memory, Flooring task.

1. INTRODUCTION

The prevalence of work-related musculoskeletal disorders (WMSDs) among construction workers is a growing concern. The United States Bureau of Labor Statistics (BLS) reported that workers in the construction industry are 1.23 times more likely to sustain WMSDs compared with workers in other industries (BLS, 2020), with the back being the most commonly affected body part. For example, floor layers experience back injuries at a rate 1.7 times higher than workers in other industry sectors resulting in an average of 26 days away from work. This leads to significant financial loss for construction firms due to workers' compensation costs. In the United States, Bhattacharya (2014) reported that more than US$400 million is expended annually on construction workers' compensation due to WMSDs. In severe situations, back injuries could result in permanent disability and premature exit from the workforce (Nihar Gonsalves et al., 2023).

Exoskeletons are emerging as a potential solution to WMSDs, particularly back-support exoskeletons, which are wearable devices designed to support the back during work (N. Gonsalves et al., 2023; Ogunseiju et al., 2022). These devices could be broadly classified as passive or active depending on their method of augmentation. Passive back-support exoskeletons use dampers and springs to provide support to the back, while active back-support exoskeletons rely on electrical motors to provide greater support to the back (Okunola et al., 2023). These devices have been shown to reduce the risk of back injuries by decreasing muscle activity (Bosch et al., 2016), range of motion (Okunola et al., 2023), body discomfort (Gonsalves et al., 2021; Kim et al., 2019), and rate of exertion (Alemi et al., 2020; Baltrusch et al., 2021). For instance, Bosch et al. (2016) found that exoskeletons reduced back muscle activity by 35-38% during assembly work. Koopman et al. (2020) reported a 13-21% reduction in the range of motion of the back during static bending and an average of 14% during lifting tasks. Gonsalves et al. (2021) observed a 100% reduction in perceived discomfort at the back among exoskeleton users.

Despite these benefits, there are potential drawbacks to using exoskeletons in construction, such as difficulty working in confined spaces (Nussbaum et al., 2019), increased fall risks due to the weight of the device (Alabdulkarim et al., 2019; Kim et al., 2019; Massardi et al., 2023), discomfort in other body parts (N. Gonsalves et al., 2023; Gonsalves et al., 2021), restrictions in movement (Fox et al., 2019), catch and snag risks (de Looze et al., 2016; Kim et al., 2019), and thermal discomfort (Liu et al., 2021). Gonsalves et al. (2021) found that exoskeletons may cause discomfort in other parts of the body, such as the chest and thigh regions. This is because exoskeletons could redirect loading from one part of the body to another (Picchiotti et al., 2019). The devices could also be challenging to adjust to fit (N. Gonsalves et al., 2023; Gorgey, 2018), and improper adjustment can lead to uneven loading and balancing, increasing user awareness of the device and distracting from tasks and surroundings (Bequette et al., 2020; Marchand et al., 2021). These unintended consequences could increase workers' mental workload (Bequette et al., 2020).

Mental workload refers to the cognitive resources needed to perform tasks (J. Y. Chen et al., 2017). A prolonged increase in mental workload can result in distraction, emotional distress, anxiety, and stress, which can negatively affect workers' overall well-being and performance. High mental workload has been linked to performance issues that can increase the risk of accidents (Hopstaken et al., 2015; Lee et al., 2012) due to reduced ability to identify and evaluate hazards under new and varying work conditions (Alotaibi & Gambatese, 2024). To address these concerns, site managers often employ observation strategies to monitor and report the mental state of their workers while using exoskeletons (Pourmazaherian et al., 2021). However, these strategies could be subjective and time-consuming, limiting the feedback from workers (Alotaibi & Gambatese, 2024). Real-time monitoring of workers' mental workload during exoskeleton use could inform strategies to reduce the triggers, but there has been limited research on models for predicting mental workload during exoskeleton use.

Electroencephalogram is an objective method of measuring brain activity. Signals from this method are often used to infer mental workload, due to the high temporal resolution, convenience, and cost-effectiveness of the device (Cheng et al., 2022). Machine learning techniques, particularly deep learning, provide opportunities for extracting insightful features from EEG data that could be used to predict mental workload (Qin & Bulbul, 2023b). Long Short-Term Memory (LSTM) network, a type of recurrent neural network, can learn long-term dependencies between time steps of data and predict future sequences (Wang et al., 2018). LSTM network has been applied to sequential learning tasks like construction equipment activity analysis (Hernandez et al., 2019), construction workers' safety harness usage (Guo et al., 2023), mixed reality learning environments (Ogunseiju et al., 2023) and fatigue detection and early warning systems (Liu et al., 2020) that need historical time-series data for decision-making. Furthermore, combining convolutional neural networks (CNN) and LSTM could lead to better results

(Huang et al., 2022; Longo, 2022). This is because CNNs perform well at capturing spatial relationships, while LSTMs are effective at modeling temporal dependencies within individual and multiple EEG recordings (Wang et al., 2018; Zhang et al., 2021). Therefore, this study investigates the extent to which workers' mental workload due to exoskeleton use can be predicted from EEG data using the LSTM and the combination of CNN and LSTM. Using flooring tasks as a case study, this paper compares actual and predicted mental workload during work with an active back-support exoskeleton. This paper comprises six sections. After the introduction in "Section 1", "Section 2" describes the background by highlighting the evaluation of mental workload and machine learning for mental workload prediction. This is followed by Sections 3 – 6, which represent the methodology, results, discussion, and conclusion and limitation sections, respectively. The study contributes to the limited knowledge of the unintended consequences of using wearable devices like exoskeletons in construction work. The findings inform the effectiveness of different convolutional neural network variations in detecting significant features of EEG data, guiding algorithm choices for future applications. Additionally, the results shed light on the most appropriate brain channels for assessing mental workload during exoskeleton use, which can aid in the design of EEG devices that offer optimal cost-effectiveness and minimal channels while providing better explanatory power.

2. BACKGROUND

2.1 Evaluation of Mental Workload

Research indicates a relationship between mental workload, and task demand and performance (Fan & Smith, 2017). Low or high levels of mental workload can negatively impact task execution and increase error rates (Mastropietro et al., 2023). Over-concentration on a task can limit attention to other stimuli, leading to reduced vigilance and situational awareness that may expose construction workers to hazards (Chen et al., 2016). In this study, exoskeleton use may demand attention, potentially diverting mental resources needed to avoid risks such as falls and catch and snags (N. Gonsalves et al., 2023; Zhu et al., 2021). This increased mental workload can cause stress or distraction, hindering productivity and safety, making mental workload prediction a key area of interest in ergonomics (Young et al., 2015).

To assess mental workload, both subjective and objective measures have been employed. Subjective methods involve questionnaires such as the NASA Task Load Index, work profiles, and the Subjective Workload Assessment Technique (Mitropoulos & Memarian, 2013). However, these methods could be prone to errors and bias and may disrupt workers' tasks due to the time and effort required to complete them (Hwang et al., 2018). Moreover, subjective measures do not facilitate real-time data collection for mental workload prediction (Hwang et al., 2018). On the other hand, objective measures capture physiological metrics such as heart rate, pupillometry, electrodermal activity, functional magnetic resonance imaging (fMRI), functional near-infrared spectroscopy (fNIRS), and electroencephalography (EEG), providing access to real-time data (Cheng et al., 2022; Ryu & Myung, 2005). Among these, EEG is preferred for its direct measurement of brain activity from the central nervous system, unlike other metrics such as heart rate and electrodermal activity that are connected to the peripheral nervous system (Hwang et al., 2018). Also, EEG devices are portable, and suitable for mental workload assessment during construction activities (Cheng et al., 2022). Brain activity obtained from EEG is a suitable indicator of mental workload, particularly during physically demanding tasks such as construction work (Chen et al., 2016; Qin & Bulbul, 2023b).

EEG data comprises time-stamped cognitive patterns based on frequency oscillations, categorized into delta (1–4 Hz), theta (4–8 Hz), alpha (8–12 Hz), beta (13–25 Hz), and gamma (≥ 25 Hz) bands (Ke et al., 2021). These frequencies correspond to different brain states across different brain regions. For instance, the delta band is associated with deep sleep, theta with powered thinking, alpha with alertness and concentration, beta with attentional processing, and gamma with high mental activity and information processing (Ke et al., 2021). The alpha and theta frequency bands in specific brain regions are correlated with cognitive processes (Kumar & Kumar, 2016). The parietal and occipital regions of the brain play crucial roles in processing visual information (Teng & Postle, 2021). The parietal region is involved in interpreting and making sense of sensory data, including visual information (Abdurashidova et al., 2024). Meanwhile, the occipital region is key for encoding and decoding visual data (Xi et al., 2024). Also, the frontal region of the brain is essential for higher cognitive functions such as decision-making, problem-solving, planning, and emotional processing (Vaidya & Fellows, 2017; Xi et al., 2024).

Spüler et al. (2016) showed that alpha and theta activities in the parieto-occipital region are strong indicators of mental workload. Increases in mental workload correlate with increases in the frontal theta and decreases in parietal alpha activity (Käthner et al., 2014; Raufi & Longo, 2022). Changes in alpha band power in the parietal and occipital regions, and theta band power in the frontal midline, are also associated with mental workload (Sauseng et al., 2010; Spüler et al., 2016). Increased theta band power in the frontal regions of the brain has been shown to increase with the high mental workload during arithmetic operations, finger tapping, mental rotation, and lexical decision task (So et al., 2017), letter manipulation task (Itthipuripat et al., 2013) and simulated flight task (Hamann & Carstengerdes, 2022). Alpha band power in the parietal and occipital regions decreased with the increased mental workload during arithmetic problem-solving with increasing levels of difficulty (Spüler et al., 2016), text reading, and hyperlink selection (Scharinger, Kammerer, et al., 2015) and n-back task (Scharinger, Soutschek, et al., 2015). A combination of alpha and theta band power has been identified as a potential indicator of mental workload (Spüler et al., 2016). Specifically, the ratio of frontal theta to parietal and occipital alpha has been proven to be an essential physiological indicator of mental workload (Qin & Bulbul, 2023a). In other words, an increase in mental workload has been linked to an increase in frontal theta power and a reduction in parietal alpha power (Käthner et al., 2014; Raufi & Longo, 2022).

In assessing the cognitive statuses of construction workers with EEG, prior studies (Cheng et al., 2022; Ke et al., 2021; Qin & Bulbul, 2023a) have shown that EEG channels covering the frontal, temporal, parietal, and occipital regions of the brain are adequate. For instance, Qin and Bulbul (2023a) employed a 14-channel EEG device covering these four brain regions for mental workload evaluation in a construction assembly task with an augmented reality head-mounted display. Similarly, Ke et al. (2021) considered these four brain regions to measure the cognitive performance of construction workers. The ability to measure mental workload with EEG motivates the exploration of techniques for real-time prediction of mental workload. This, in turn, could open opportunities for exploring strategies for reducing mental workload due to exoskeleton use on construction sites. Machine learning has transformed the field of cognitive assessment by enabling the development of predictive models that can analyze complex and high-dimensional data.

2.2 Machine Learning for Mental Workload Prediction

Researchers have employed machine learning algorithms, including supervised and deep learning classifiers, to predict brain activity for a range of purposes such as learning and monitoring workforce health. For example, Dimitrakopoulos et al. (2017) used support vector machines to assess performance levels during arithmetic tasks using EEG data, while Zarjam et al. (2015) employed an artificial neural network to forecast workload levels during a mental arithmetic addition task based on EEG data. In construction, Jebelli et al. (2018a) similarly used a support vector machine to categorize stress levels in construction workers using EEG data. Despite the high performance of the resulting models, supervised learning techniques often involve manual feature extraction, which can be time-consuming and less suitable for real-time data analysis when assessing mental workload (Liu et al., 2019; Wang et al., 2023). In addition, EEG data can present challenges due to their low signal-to-noise ratio, making effective feature extraction difficult (Iftikhar et al., 2018).

Deep learning algorithms, in contrast, automatically learn features from data, removing the need for manual processing. Unlike traditional machine learning, deep learning employs multi-layer models, allowing for a more advanced representation of the dataset (Wang et al., 2018). While deep learning models may require longer training times, they typically outperform simpler artificial neural networks (ANNs). Deep learning architectures include convolutional neural networks (CNNs) and recurrent neural networks (RNNs) (Mathew et al., 2021). CNNs are multi-layer feedforward artificial neural networks that process data to capture spatial and temporal dependencies (Wang et al., 2018; Zhang et al., 2021). They achieve this by stacking convolutional and pooling layers to learn features. In contrast, RNNs are deep learning models often employed for predicting sequential data (Staudemeyer & Morris, 2019; Wang et al., 2018). Each RNN unit features recurrent connections that enable the network to retain information over extended periods, allowing for the detection of patterns in sequential data (Wang et al., 2018). However, traditional RNNs like the Elman Network can be time-consuming to train and challenging due to the vanishing and exploding gradient problems (Van Houdt et al., 2020). Advanced architectures such as long short-term memory (LSTM) networks have been developed to address these challenges. LSTM uses a memory block consisting of input, output, and forget gates (Yusuf et al., 2023). This structure enables each recurrent unit to capture long-term relationships across different time scales, making LSTM effective for predicting complex time sequence data, such as EEG data. As a result, LSTM has been used in various contexts for predicting mental

workload. For example, Yoo et al. (2023) and Yusuf et al. (2023) leveraged LSTM to develop a model for predicting cognitive load from EEG data. Zhang (2022) used LSTM to evaluate mental workload evaluation during an envisioning task. In construction, Qin and Bulbul (2023b) used LSTM on EEG data captured during a framing task to predict mental workload.

EEG signals contain intricate spatial and temporal patterns that are challenging to capture using manually engineered features and conventional machine learning algorithms (Jenke et al., 2014). Therefore, mental workload prediction often requires considering both spatial and temporal dependencies in EEG data (Cebecí et al., 2020; Varatharajah et al., 2017). CNNs are effective at capturing spatial relationships within individual EEG recordings, while LSTMs excel at capturing temporal dependencies across multiple EEG recordings (Wang et al., 2018; Zhang et al., 2021). In CNN-LSTM, by combining both CNN and LSTM, the model can leverage the complementary strengths of each component where CNN can be used for local features extractions from sequential data while LSTM can be employed to handle sequence and long-term temporal dependencies, enhancing prediction accuracy (Zhang et al., 2021; Zhao et al., 2017). Huang et al. (2022) compared XGBoost, CNN, LSTM, and CNN-LSTM in assessing mental workload among drivers. The study reported better performance with CNN-LSTM. Longo (2022) used CNN-LSTM in modeling mental workload and predicting brain rate from EEG data. The study reported that predictions by CNN-LSTM are better than those by CNN. Despite the potential of LSTM and CNN-LSTM for forecasting EEG data, limited studies have investigated their use in predicting mental workload during exoskeleton use in construction. Furthermore, there is limited understanding of how effective these classifiers are in forecasting mental workload during exoskeleton use. Therefore, this study explores the prediction of the mental workload of construction workers from EEG data using the LSTM and the combination of CNN and LSTM during exoskeleton use.

3. METHODOLOGY

This section describes the procedure employed to achieve the objective of the study including the experimental design to collect brain activity of participants performing flooring tasks with an exoskeleton, preprocessing of the brain activity data, and prediction of mental workload using the data (Figure 1).
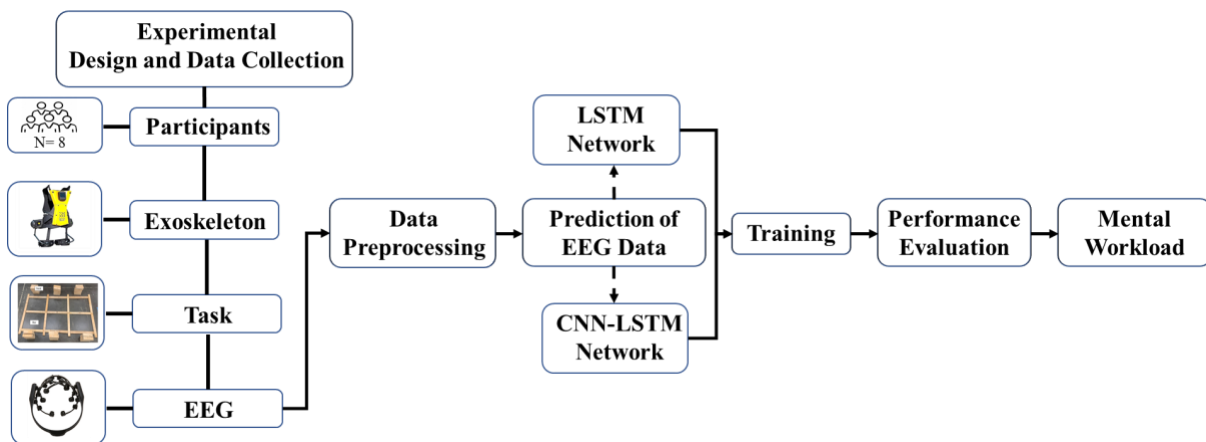

Figure 1: Overview of the research methodology.

3.1 Experimental Design and Data Collection

3.1.1 Participants

Eight male graduate students (N = 8) were recruited to perform a simulated flooring task with an active back-support exoskeleton. Similar sample sizes have been used in previous studies (Poliero et al., 2020; Wei et al., 2020). The average age, weight, and height of participants is 30 years, 79.8 kg, and 1.84 m respectively. None of the participants reported any prior musculoskeletal injury that could impact their participation in the study.

3.1.2 Exoskeleton

The active exoskeleton used for the study is Cray X shown in Figure 2. The Cray X, from German Bionic, weighs 7kg and can provide a lifting support of about 30kg. Cray X consists of a frame and strap pads of different sizes for the legs, chest, shoulders, and waist. The frame includes a 40V battery and motor. The exoskeleton provides different levels of support for bending, lifting, placing, and walking.

Figure 2: Active (CrayX) back-support exoskeleton.

3.1.3 Task

The flooring task involved lifting, placing, and installing 20-floor tiles in each bay of a wooden frame comprising six bays. Each bay can fit 20 floor tiles (Figure 3). The participants were asked to lift and place 20 timber tiles (10kg) beside each bay, and subsequently install the stacked tiles in each bay. Each tile weighs 0.5kg. A cycle of the flooring task includes lifting, placing, and installation of the timber floor tiles (20) in each bay. The task comprises six cycles given that the participants installed the tiles in six bays. Before commencing the tasks, the participants received instructions on how to perform the task. The participants performed the flooring task with an active back-support exoskeleton while wearing an EEG headset (see Section 3.1.4).
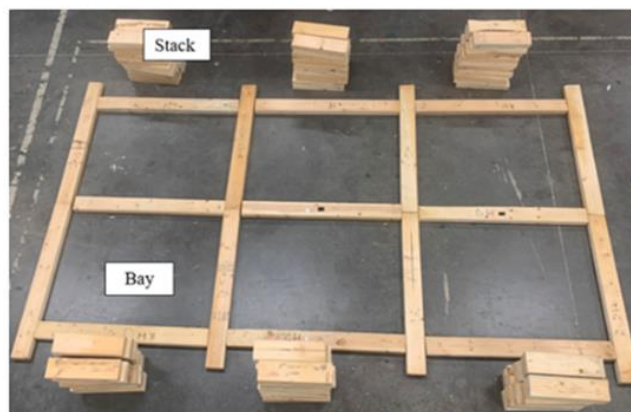

Figure 3: Experimental layout of the simulated flooring task.

3.1.4 EEG Device

Emotiv EPOC+, a wireless EEG headset, was used in this study to collect brain activity (see Table 1) while performing the flooring task described in Section 3.1.3. The EEG device records the electrical activity of the brain through contact between electrodes embedded in various portions of the headset and the scalp. The electrodes capture activations in channels located in four regions of the brain such as the frontal, temporal, parietal, and occipital regions (Figure 4). The channels in these regions are shown in Table 1. The headset also has 2 reference electrodes (DMS and DRL) located on the P3 and P4 channels following the 10-20 international EEG system. Data from these channels were captured at a frequency of 128 Hz. Researchers have used wireless headsets for similar studies due to their lightweight design and affordability (Cheng et al., 2022).

Table 1: Emotiv EPOC-Plus, Brain regions, and channels.

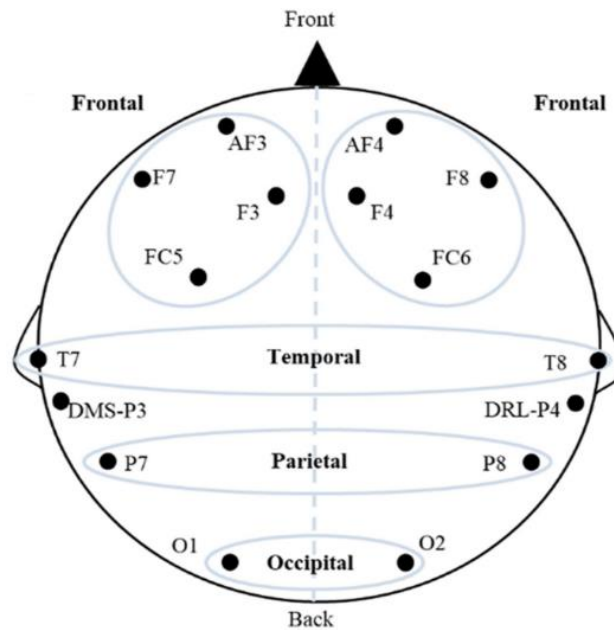| Emotiv EPOC-Plus	Brain Regions	Channels
	Frontal lobe	AF3, AF4, F3, F4, FC5, FC6, F7, and F8
	Temporal lobe	T7 and T8
	Parietal lobe	P7 and P8
	Occipital lobe	O1 and O2

Figure 4: Electrode Location on Scalp (Ke et al., 2021).

3.2 Data Preprocessing

EEG data are susceptible to contamination from intrinsic and extrinsic artifacts, particularly when subjects are engaged in physical activities like construction work (Jebelli et al., 2018b). These artifacts impact the quality of the signals. Intrinsic artifacts are triggered by movements such as eye blinking and muscle movement, while extrinsic artifacts are caused by external influences such as noise from wires and electrode popping. This study used the framework proposed by Jebelli et al. (2018b) to reduce the artifacts in the EEG data obtained from the simulated task. The EEG data were fed into EEGLAB, a MATLAB toolbox for processing physiological data (Delorme & Makeig, 2004). The extrinsic artifacts were removed using a Bandpass filter with cut-off frequencies of 0.5 and 65 Hz (Jebelli et al., 2018b). Another extrinsic artifact due to noise from wires was removed using a notch filter applied at a frequency of 60Hz. The intrinsic artifacts were removed using independent component analysis (ICA) (Mantini et al., 2008). The EEG data was decomposed using the Extended Infomax method into 14 components, representing the 14 channels of the EEG device, and displayed using a scalp heatmap to reject the intrinsic artifacts (Frølich & Dowding, 2018). Preprocessed data from eight (8) channels were utilized for this study. This includes channels AF3, AF4, F3, and F4 positioned in the frontal-mid region, channels O1 and O2 located in the occipital region, and channels P7 and P8 located in the parietal region of the scalp. As explained in Zection 2.1, studies have shown that these brain regions have strong correction with mental workload (Hamann & Carstengerdes, 2022; So et al., 2017; Spüler et al., 2016).

3.3 Prediction of EEG Data

3.3.1 Long short-term memory network

LSTM network was used in this study to forecast subsequent values of EEG data based on the preprocessed data obtained from Section 3.2. LSTM neural network processes data by iterating over current time steps and retaining useful information to help with the processing of new data points. The regression LSTM neural network consists of four layers: an input layer, the LSTM layer, the fully connected layer, and a regression layer (Yusuf et al., 2023). The input layer accepts the input time-series data and transfers this to the LSTM layer. The LSTM layer comprises a cell, an input gate, an output gate, and a forget gate. The LSTM layer comprises a cell, an input gate, an output gate, and a forget gate (Staudemeyer & Morris, 2019). The cell stores long-term time-series data and uses the gates to control the flow of the data within and out of the cell. The forget gate decides which information should be ignored in the cell (Van Houdt et al., 2020). The LSTM layer comprises 128 hidden units. The number of hidden units determines how much information or data is learned by the layer. More hidden units could result in better results but are more likely to result in overfitting of the training data. This is addressed through regularization (e.g., dropout) and early stopping during training (Moon et al., 2015; Wu et al., 2021). The fully connected layer does the discriminative learning in the LSTM network. It learns weights that can identify features in the training data. The regression layer determines the performance metrics needed for the prediction task. The process involved in the LSTM operation is illustrated in Equations (1) to (5), where b and W are bias vectors and weight matrices, respectively. The function σ refers to the sigmoid function. The forget gate layer, denoted as f_t, controls how much prior information from h_{t-1} is combined with p_t. When f_t is equal to 1, the model retains the previous information, while a value of 0 means that the model discards it entirely. The input gate layer, i_t, selects which data to preserve in the cell state c_t, working in conjunction with p_t. The output layer determines the information to be released and processed, involving the cell state c_t and filtered input O_t. The LSTM hidden state h_t is updated at every time step t. The variable p_t encompasses key aspects of power production predictions, such as the output of the pooling layer at time t and serves as an input to the LSTM memory cell. Figure 5 depicts the LSTM architecture.

$$i_t = \sigma\left(W_{pi}p_t + W_{hi}h_{t-1} + W_{hi}c_{t-1} + b_i\right) \qquad \text{Equation (1)}$$

$$f_t = \sigma\left(W_{pf}p_t + W_{hf}h_{t-1} + W_{cf}c_{t-1} + b_f\right) \qquad \text{Equation (2)}$$

$$O_t = \sigma\left(W_{po}p_t + W_{ho}h_{t-1} + W_{co}c_t + b_o\right) \qquad \text{Equation (3)}$$

$$C_t = f_t * C_{t-1} + i_t * \sigma\left(W_{pc}p_t + W_{hc}h_{t-1} + b_c\right) \qquad \text{Equation (4)}$$

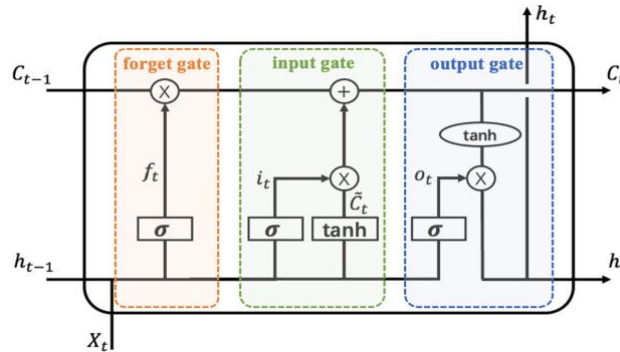$$h_t = O_t * \sigma(C_t) \qquad \text{Equation (5)}$$

Figure 5: LSTM architecture.

3.3.2 CNN-LSTM

In addition to the LSTM network described in Section 3.3.1, the performance of the CNN-LSTM was evaluated. The CNN-LSTM (Figure 6) combines CNN layers with LSTM layers. This combined architecture aims to leverage the strengths of both models to improve the prediction performance for EEG data. The architecture consists of an input layer, two 1D convolutional layers with a kernel size of 5 and 32 filters, two Batch Normalization (BN), and rectified linear unit (ReLU) activations layers. The input layer serves as the entry point for the input data. The Batch Normalization layer normalizes the input data, improving training stability and performance. The ReLU

activation layer introduces non-linearity and helps the network learn complex relationships in the data. The learned relationships are accepted by the LSTM layer (similar to that described in Section 3.3.1) which captures temporal dependencies in the data. The LSTM layer is followed by a fully connected layer and regression layer. The fully connected layer maps the output of the LSTM layer to the desired output size, which is equal to the number of channels in the input data. The regression layer serves as the output layer for the predicted EEG data.
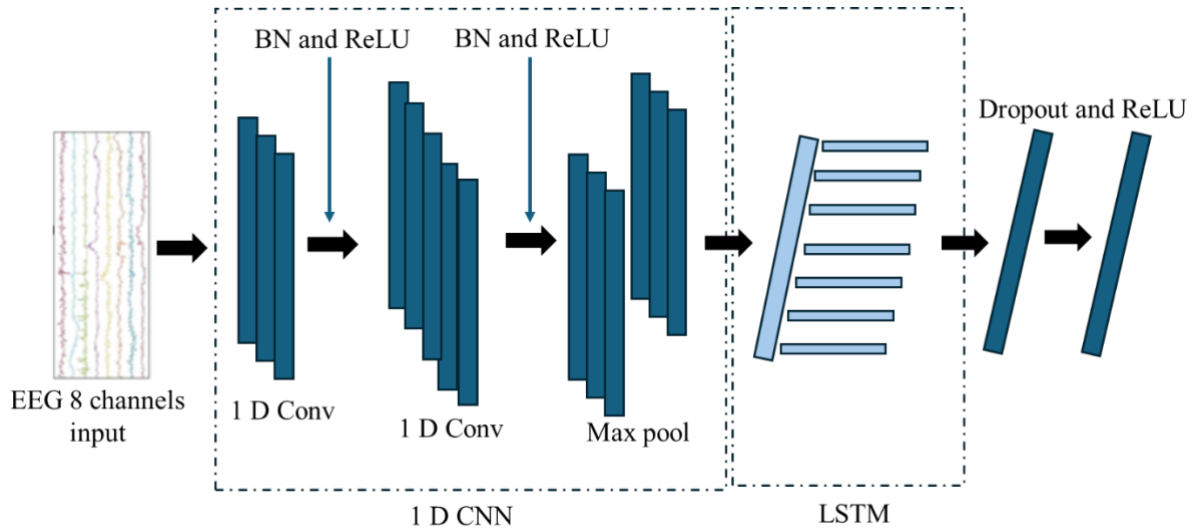

Figure 6: CNN-LSTM architecture (Adapted from Qin et al. (2024)).

3.3.3 Training LSTM and CNN-LSTM

The LSTM and CNN-LSTM networks were trained with the preprocessed time-series EEG data from the channels mentioned in Section 3.2 to output future time steps of EEG values. The training was conducted using MATLAB R2023a, installed on a machine with NVIDIA GeForce RTX 3080 GPU and 32GB memory. The EEG data from these channels were initially split into training, validation, and testing, accounting for 70%, 10%, and 20% of the data respectively. To address concerns such as overfitting and training divergence, both the predictors and targets were normalized to zero mean and unit variance (Srivastava et al., 2014). The choice of hyperparameters plays a crucial role in determining the performance of models (Arnold et al., 2024). Consequently, in this study, the Adam optimizer, an extension of stochastic gradient descent, with a batch size of 128 using a mean-squared loss function was used for the training (Kingma & Ba, 2014). This ensures that the learning steps during training are scale-invariant to parameter gradients. Additionally, employing the same padding helped retain the features of the EEG signals during the convolution process, preventing the loss of valuable information. Additionally, 200 epochs were employed, along with a learning rate of 0.001. These hyperparameters were selected to optimize the training process and enhance the performance of the LSTM and CNN-LSTM networks.

3.3.4 Performance evaluation

The performance of the LSTM and CNN-LSTM models was evaluated using the Root Mean Square Error (RMSE) and R-squared. RMSE is a standard statistical metric for computing accuracy. RMSE is generally used to evaluate the difference between the actual and predicted values from the model. RMSE is sensitive to large and substantial errors compared to other metrics like mean absolute error because the squared term in the formula (Equation 6) emphasizes greater errors exponentially than smaller ones (Persson & Ståhl, 2020). RMSE can be determined with Equation (6), where A_i and P_i are the actual and predicted EEG datasets respectively, and n is the number of EEG datasets. The lower the RMSE, the better a model would fit a dataset. However, given that RMSE could be misleading if some features are not normally distributed or if there is uncertainty in data (Hodson, 2022), R-squared was also determined (See Equation 7). The R-squared (R^2), coefficient of determination, which indicates the goodness-of-fit and describes the variance in the response of a regression model, was computed following Renaud and Victoria-Feser (2010). The R^2 value ranges from 0 to 1. The higher the R^2 value, the better a model fits a dataset.

$$RMSE = \sqrt{\sum(P_i - A_i)^2}/n \qquad \text{Equation (6)}$$

$$R^2 = 1 - \frac{\sum(p_i - a_i)^2}{\sum(p_i - a_i)^2} \qquad \text{Equation (7)}$$

3.4 Mental workload

After predicting the EEG data, the mental workload of the actual (preprocessed) EEG data (from Section 3.2) and the predicted EEG data from Section 3.3.1 were determined. First, this was achieved by computing the dataset's power spectral density using the Welch Method (J. Chen et al., 2017). Power spectral density (PSD) represents the power of the EEG signal at different frequency bands and is useful for assessing different states of cognitive functions (Kumar & Kumar, 2016). The Welch method involves dividing EEG signals of length L into M overlapping segments. The modified periodogram for each segment was then calculated using a Hamming window. Subsequently, the periodograms were averaged to alleviate the variance of the resulting PSD estimates. The expression for the Welch method in computing PSD for each N-point time series in the mth segment (out of M segments) is represented by Chiu et al. (2023) as follows:

$$P_{x_m,M}(f) = \frac{1}{N}\left|\sum_{n=0}^{N-1} x_m(n)e^{-\frac{j2\pi nk}{N}}\right|^2 \qquad \text{Equation (8)}$$

The PSD for the entire series, P_w, can be expressed as:

$$P_w(f) = \frac{1}{M}\sum_{m=0}^{M-1} P_{x_m,M}(f) \qquad \text{Equation (9)}$$

Where P_x is the Power spectral density; M is the Number of segments; m is the Segment index; N is the length of each segment; n is the Sample index; k is the Normalizing constant; and f is the Frequency variable.

Secondly, the relative band power of the windowed or segmented data in theta and alpha frequency bands was determined from the PSD values. Researchers have identified theta and/or alpha power as suitable indicators of mental workload (Scharinger, Soutschek, et al., 2015; Spüler et al., 2016). Lastly, the mental workload of each segment was determined by dividing the mean power in the theta band of the frontal channels (AF3, AF4, F3, and F4) with the mean power in the alpha band of the occipital (O1 and O2), and parietal alpha channels (P7 and P8) using Equation 10. The approximate spectral limits of the theta and alpha frequency bands are 4–8 Hz and 8–14 Hz respectively (Simon et al., 2011).

$$MW(t) = \frac{\theta f(t)}{\alpha p(t)} \qquad \text{Equation (10)}$$

Where, MW(t) denotes the mental workload at time t, and θf(t) and αp(t) are the mean spectral power of frontal theta and occipitoparietal alpha rhythms at time t respectively.

4. RESULTS

This section presents the performance of the LSTM and the CNN-LSTM models represented by the RMSE and R^2 scores, and the mental workload. The mental workload shows the comparison between the predicted and actual PSD values, the average power, and the comparison between the predicted and actual mental workload.

4.1 Performance of the LSTM and CNN-LSTM Models

Figures 7 and 8 illustrate the RMSE and R^2 values, respectively, for the EEG channels of the test data in the LSTM and CNN-LSTM models. It can be observed that the LSTM model outperformed the CNN-LSTM model across all the channels. Channels P7 and AF3 have the lowest RMSE of 0.1147 and 0.1267 respectively. A previous study has indicated that a RMSE value closer to zero gives a better predictive power (Miyamoto et al., 2022). In the LSTM model, the lowest RMSE values in the frontal, parietal, and occipital lobes were recorded in channels AF3 (0.127), P7 (0.115), and O1 (0.130), respectively. For the CNN-LSTM model, the lowest RMSE values in the frontal, parietal, and occipital lobes can be observed in channels AF3 (0.418), P8 (1.069), and O1 (1.013), respectively. Overall, the RMSE values were higher across all channels in the CNN-LSTM model compared to the LSTM model, a trend also observed when considering the overall brain regions.
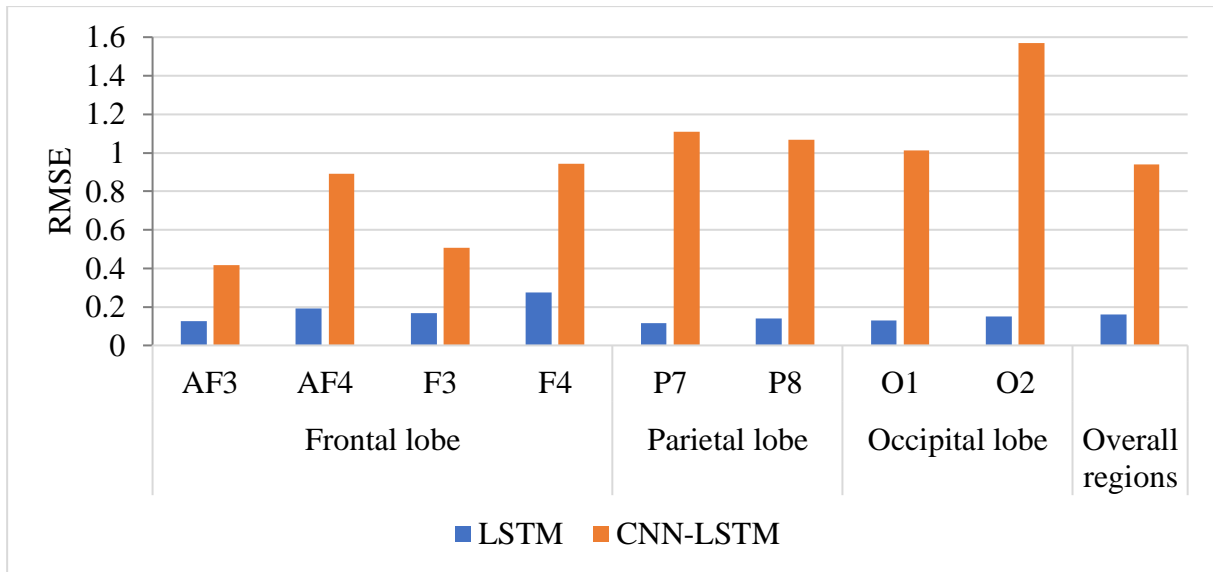
Figure 7: RMSE for LSTM and CNN-LSTM models.

As shown in Figure 8, the LSTM model consistently achieved R^2 values of more than 0.8 across all channels. The highest R^2 values in the LSTM model were in channels AF4 (0.963) in the frontal lobe, P7 (0.992) in the parietal lobe, and O2 (0.992) in the occipital lobe. In contrast, the CNN-LSTM model's highest R^2 values were found in channels AF4 (0.447) in the frontal lobe, P8 (0.726) in the parietal lobe, and O2 (0.218) in the occipital lobe, respectively. The R^2 values of the overall brain regions for the LSTM model were higher than the R^2 values of the CNN-LSTM model.
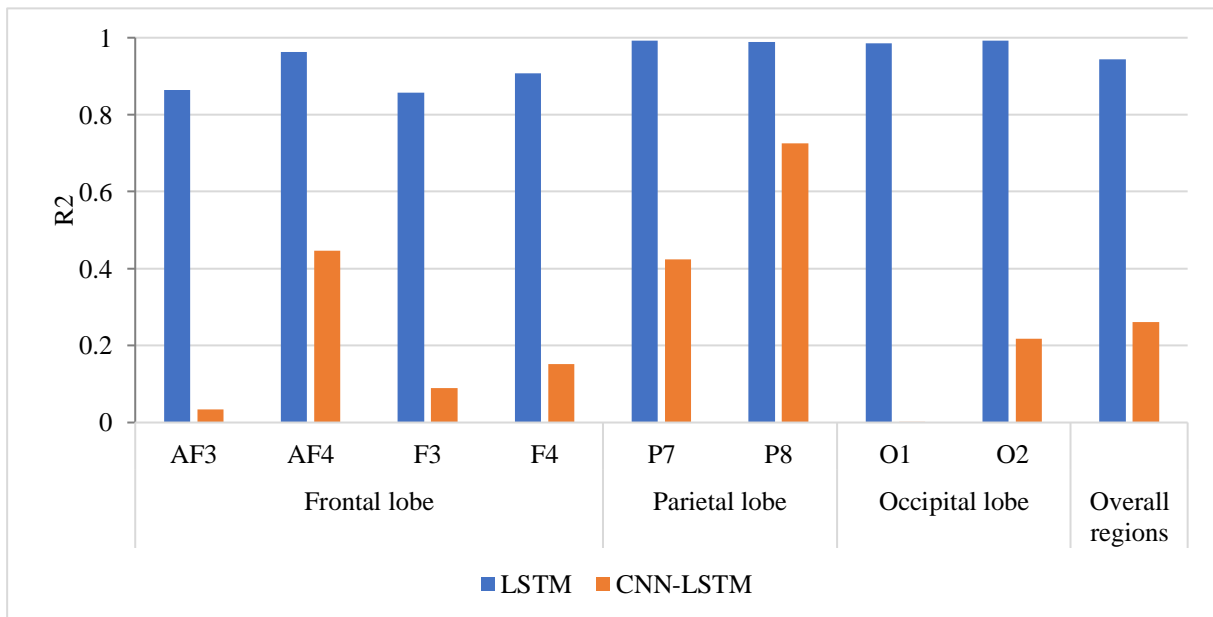

Figure 8: R^2 for LSTM and CNN-LSTM models.

4.2 Mental workload

4.2.1 Comparison between predicted and actual PSD

Figures 9a-e show the predicted (i.e., using the LSTM model) and actual power spectral density of the AF3, AF4, O1, O2, and P7 EEG channels for the data of the test participants. These five EEG channels have the lowest RMSE

and the highest R^2 values with the LSTM model. The predicted and actual data are represented with the red and blue lines, respectively. Figure 9a-e indicates that at less than 20Hz the EEG channels (i.e., AF3, AF4, O1, O2, and P7) show some consistency between the predicted and actual PSD values for the theta (4 - 8 Hz), and alpha (8 - 12 Hz) frequency bands.
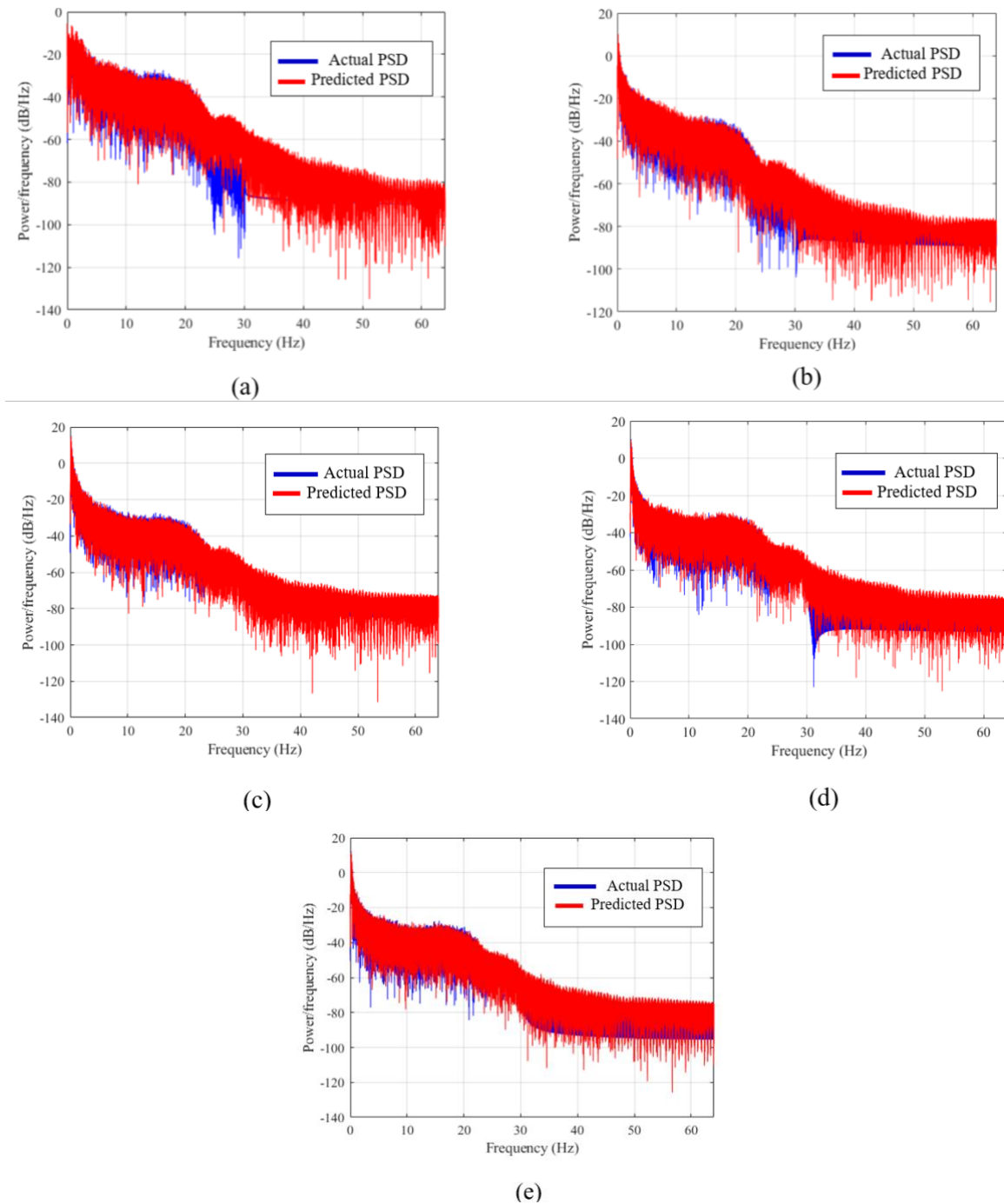

Figure 9: Predicted and actual power spectral density of the (a) AF3, (b) AF4 (c) O1 (d) O2, and (e) P7 channels.

4.2.2 Average power

The actual and predicted average spectral power for the eight (8) EEG channels are shown in Figure 10. The predicted and actual average spectral power for the eight (8) EEG channels is presented based on the theta (4 - 8 Hz), and alpha (8 - 12 Hz) frequency bands. Figure 10 indicates that in the theta frequency band, there were major

differences in the actual and predicted average spectral power in the F4 (17.6%), P8 (40.4%), and O1 (65.1%) channels. Similarly, in the alpha frequency band, the major differences in the actual and predicted average spectral power were noticed in the AF4 (50.8%), F3 (31.6%), P8 (56.7%), and O1 (86%) channels.
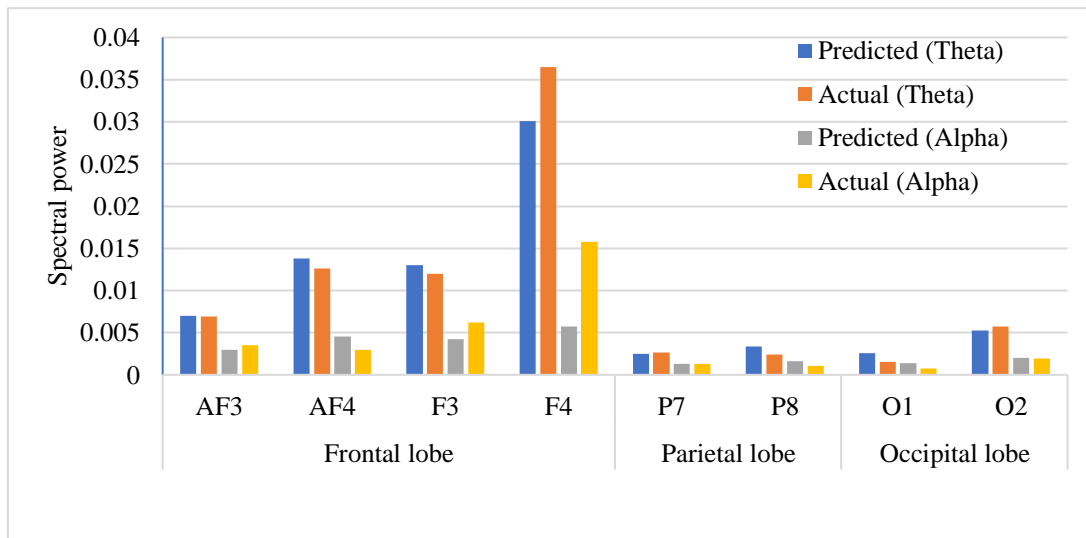

Figure 10: Predicted and actual spectral power.

4.2.3 Comparison between predicted and actual mental workload

The extent to which mental workload due to exoskeleton-use can be predicted is illustrated in the scatter diagram in Figure 11. The plot has an R^2 score of 0.7485 indicating a strong correlation between the predicted and the actual mental workload.
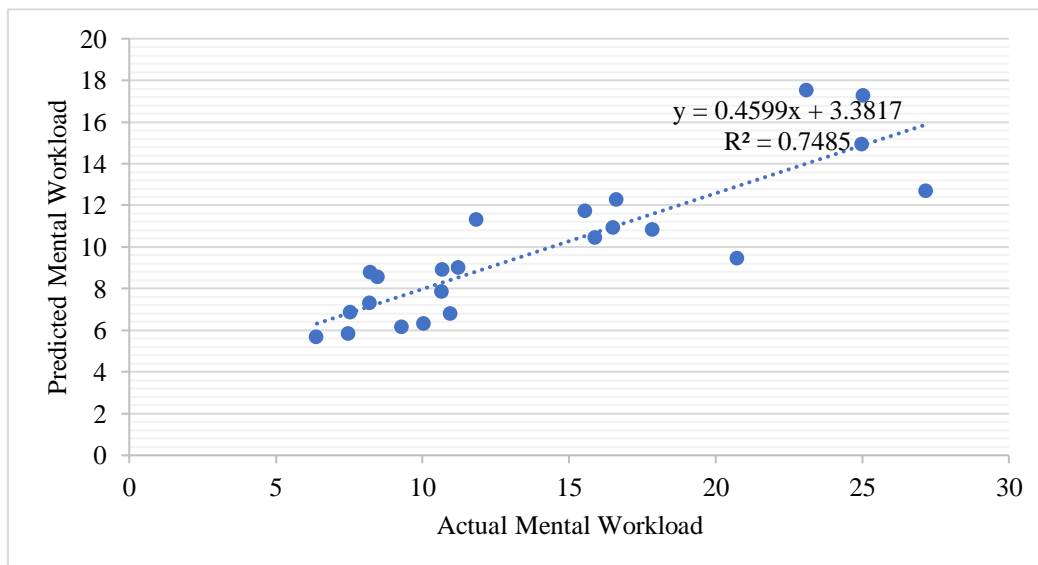

Figure 11: Comparison of predicted and actual values of the mental workload.

5. DISCUSSION

This section discusses the insights obtained from the results and the implications of the findings. The study discusses the performance of the LSTM and CNN-LSTM models and the prediction of the mental workload of exoskeleton users.

5.1 Performance of the LSTM and CNN-LSTM Models

The comparison between the LSTM and CNN-LSTM models demonstrates that the LSTM model outperforms the CNN-LSTM model across all EEG channels in terms of both RMSE and R² values. The LSTM model achieved an average RMSE of 0.16 and an average R² of 0.94, while the CNN-LSTM model attained an average RMSE of 0.94 and an average R² of 0.26 across all channels. Since RMSE measures the difference between actual and predicted EEG signals, the lower RMSE in the LSTM model indicates minimal discrepancies between the actual and predicted EEG values (Chicco et al., 2021). The higher R² values of the LSTM model further reveal its ability to explain a greater proportion of variance in the actual EEG data compared to the CNN-LSTM model. In contrast, the higher RMSE values observed in the CNN-LSTM model suggest that this hybrid approach may not be as effective in capturing the complexities of EEG data for mental workload prediction. The additional complexity introduced by combining two models may not have been necessary or beneficial in this context, as shown by its suboptimal performance compared to the LSTM model alone. This study also identified the EEG channels whose activity can be predicted with reduced errors. Channels in the frontal (AF3 and AF4), occipital (O1 and O2), and parietal (P7) lobes had the lowest RMSE and the highest R^2 values with the LSTM model. These channels have been shown in previous studies (So et al., 2017; Spüler et al., 2016) to have strong correlations with mental workload. These findings have practical applications in construction as accurate prediction of brain activity is essential for optimizing the use of exoskeletons and identifying potential safety risks (Chen et al., 2016; Qin & Bulbul, 2023b). By proactively managing mental workload, construction firms can enhance worker safety and productivity. The study highlights the potential of LSTM for monitoring and predicting mental workload in construction settings, providing a reliable tool for improving the safety and well-being of workers relying on exoskeletons.

5.2 Mental Workload

The study identified the best-performing EEG channels in predicting mental workload. Specifically, the frontal (AF3 and AF4), occipital (O1 and O2), and parietal (P7) lobes were found to be effective in the mental workload predictive model. These channels align with previous studies indicating strong correlations between these brain regions and mental workload (Alpizar et al., 2020). The identified channels in this study could help in designing EEG devices that provide optimal cost-effectiveness with better explanatory power and minimum channels (Wang et al., 2017). The overlap observed between the predicted and actual power spectral density (PSD) in the theta and alpha frequency bands for each examined EEG channel (AF3, AF4, O1, O2, and P7) confirms the effectiveness of the LSTM model in capturing patterns related to mental workload (Spüler et al., 2016). These bands are known for indicating mental workload and cognitive states such as alertness and relaxation (Kumar & Kumar, 2016; Sauseng et al., 2010; Spüler et al., 2016). However, discrepancies between predicted and actual PSD begin to emerge in the beta and gamma band regions at frequencies over 20 Hz in most of the channels. This suggests that higher frequency bands may present challenges in prediction and warrant further investigation in future research. Furthermore, the strong correlation (R² = 0.7485) between predicted and actual mental workload highlights the LSTM model's reliability in forecasting cognitive load during exoskeleton use. This finding supports previous studies asserting the feasibility of predicting mental workload (Borghini et al., 2014; Missonnier et al., 2006; Qin & Bulbul, 2023b).

These results have practical applications for the construction industry. Accurate prediction of mental workload can inform decisions on task assignments, work schedules, and breaks, optimizing worker performance and minimizing safety risks (Chen et al., 2016; Cheng et al., 2022; Qin & Bulbul, 2023b). Proactive management of mental workload can enhance worker safety and productivity (Chen et al., 2016; J. Y. Chen et al., 2017), contributing to more sustainable and effective use of exoskeletons in construction. The findings provide valuable insights into the potential of machine learning models like LSTM for monitoring and predicting mental workload in construction settings. This holds promise for improving the safety and well-being of construction workers using exoskeletons for physically demanding tasks. Future research could continue to explore the use of these EEG channels and frequency bands in predicting mental workload, especially at higher frequencies, to further improve the accuracy and applicability of these models.

6. CONCLUSIONS AND LIMITATIONS

This study presents the extent to which mental workload due to exoskeleton use can be predicted from EEG data using LSTM and CNN-LSTM networks. EEG data were obtained from an experimental study where participants performed flooring tasks with an active back-support exoskeleton. The data were preprocessed and trained with the LSTM and the hybrid CNN-LSTM network. The study showed that the LSTM network *(avg. RMSE = 0.16, avg. R^2 = 0.94)* outperformed the CNN-LSTM network *(avg. RMSE = 0.94, avg. R^2 = 0.26)*. A comparison of the actual and predicted power spectral density indicates good consistency in all the EEG channels in the theta and alpha frequency bands. About 75% variance in the actual mental workload was captured in the prediction. The results of this study contribute to the limited literature on the impact of unintended consequences of using exoskeletons for construction work. This research adds to the limited literature on the unintended consequences of using exoskeletons in construction work. It may motivate further studies on using deep learning for real-time mental workload prediction when employing other technological interventions in construction projects. The findings provide insights into the effectiveness of various convolutional neural network variations for identifying key features of EEG data, which can guide future algorithm selections. Moreover, the results offer insights into the most suitable brain channels for assessing mental workload during exoskeleton use, supporting the development of EEG devices that balance cost-effectiveness and explanatory power with minimal channels.

The study may have been limited due to the sample size of eight participants which was used to train the deep learning models. Training data with a larger sample could improve the performance of the model and enhance its generalizability. Future studies could consider a larger sample size to enhance the generalizability of the findings. Future studies can also explore the use of other deep learning models or hybrid approaches to generate accurate and robust models for advancing mental workload prediction in exoskeleton use. In addition, the performance of other time-series-based data augmentation techniques such as scaling, permutation, and generative adversarial networks, in generating synthetic data could be explored. Given the performance of LSTM, future research could also explore the application of LSTM models in real-time monitoring of mental workload during exoskeleton use. Additionally, further investigation into the factors influencing the performance of different models can provide valuable insights for enhancing prediction accuracy and ensuring safe and effective exoskeleton use in various work environments. This study focused on active back-support exoskeleton. Future studies could explore the extent to which similar prediction models could be developed for passive back-support exoskeletons. Comparison of the performance of the prediction models could inform if different models would be needed or if similar models would work for both exoskeleton types.

ACKNOWLEDGEMENT

REFERENCES

Abdurashidova, K., Rajabov, F., Karimova, N., & Akbarova, S. (2024). Visual-Sensory Information Processing Using Multichannel EEG Signals. In B. J. Choi, D. Singh, U. S. Tiwary, & W.-Y. Chung, Intelligent Human Computer Interaction International Conference on Intelligent Human Computer Interaction, Cham. https://doi.org/10.1007/978-3-031-53827-8_7

Alabdulkarim, S., Kim, S., & Nussbaum, M. A. (2019). Effects of exoskeleton design and precision requirements on physical demands and quality in a simulated overhead drilling task. Applied ergonomics, 80, 136-145. https://doi.org/10.1016/j.apergo.2019.05.014

Alemi, M. M., Madinei, S., Kim, S., Srinivasan, D., & Nussbaum, M. A. (2020). Effects of Two Passive Back-Support Exoskeletons on Muscle Activity, Energy Expenditure, and Subjective Assessments During Repetitive Lifting. Human Factors, 62(3), 458-474. https://doi.org/10.1177/0018720819897669

Alotaibi, A., & Gambatese, J. (2024). Impact of Task Demand and Physical Energy on Mental Workload Experienced by Construction Workforce: Insights of Construction Professionals. Practice Periodical on Structural Design and Construction, 29(2), 04024006. https://doi.org/10.1061/PPSCFX.SCENG-1422

Alpizar, D., Adesope, O. O., & Wong, R. M. (2020). A meta-analysis of signaling principle in multimedia learning environments. Educational Technology Research and Development, 68(5), 2095-2119. https://doi.org/10.1007/s11423-020-09748-7

Arnold, C., Biedebach, L., Küpfer, A., & Neunhoeffer, M. (2024). The role of hyperparameters in machine learning models and how to tune them. Political Science Research and Methods, 10.1017/psrm.2023.61, 1-8. https://doi.org/10.1017/psrm.2023.61

Baltrusch, S. J., Houdijk, H., van Dieen, J. H., & de Kruif, J. T. C. M. (2021). Passive Trunk Exoskeleton Acceptability and Effects on Self-efficacy in Employees with Low-Back Pain: A Mixed Method Approach. Journal of Occupational Rehabilitation, 31(1), 129-141. https://doi.org/10.1007/s10926-020-09891-1

Bequette, B., Norton, A., Jones, E., & Stirling, L. (2020). Physical and cognitive load effects due to a powered lower-body exoskeleton. Human Factors, 62(3), 411-423. https://doi.org/10.1177/0018720820907450

Bhattacharya, A. (2014). Costs of occupational musculoskeletal disorders (MSDs) in the United States. International Journal of Industrial Ergonomics, 44(3), 448-454. https://doi.org/10.1016/j.ergon.2014.01.008

BLS. (2020). Occupational injuries and illnesses resulting in musculoskeletal disorders (MSDs). United States Department of Labor. Retrieved 12/17/2023 from https://www.bls.gov/iif/nonfatal-injuries-and-illnesses-tables

Borghini, G., Astolfi, L., Vecchiato, G., Mattia, D., & Babiloni, F. (2014). Measuring neurophysiological signals in aircraft pilots and car drivers for the assessment of mental workload, fatigue and drowsiness. Neuroscience and Biobehavioral Reviews, 44, 58-75. https://doi.org/10.1016/j.neubiorev.2012.10.003

Bosch, T., van Eck, J., Knitel, K., & de Looze, M. (2016). The effects of a passive exoskeleton on muscle activity, discomfort and endurance time in forward bending work. Applied ergonomics, 54, 212-217. https://doi.org/10.1016/j.apergo.2015.12.003

Cebecí, B., Akan, A., Sütçübaşi, B., & Demıralp, T. (2020). EEG Based Mental Workload Estimation System. 2020 28th Signal Processing and Communications Applications Conference (SIU), https://doi.org/10.1109/SIU49456.2020.9302362

Chen, J., Qiu, J., & Ahn, C. (2017). Construction worker's awkward posture recognition through supervised motion tensor decomposition. Automation in Construction, 77, 67-81. https://doi.org/10.1016/j.autcon.2017.01.020

Chen, J. Y., Song, X. Y., & Lin, Z. H. (2016). Revealing the "Invisible Gorilla" in construction: Estimating construction safety through mental workload assessment. Automation in Construction, 63, 173-183. https://doi.org/10.1016/j.autcon.2015.12.018

Chen, J. Y., Taylor, J. E., & Comu, S. (2017). Assessing Task Mental Workload in Construction Projects: A Novel Electroencephalography Approach. Journal of Construction Engineering and Management, 143(8). https://doi.org/10.1061/(ASCE)CO.1943-7862.0001345

Cheng, B., Fan, C., Fu, H., Huang, J., Chen, H., & Luo, X. (2022). Measuring and computing cognitive statuses of construction workers based on electroencephalogram: a critical review. IEEE Transactions on Computational Social Systems, 9(6), 1644-1659. https://doi.org/10.1109/TCSS.2022.3158585

Chicco, D., Warrens, M. J., & Jurman, G. (2021). The coefficient of determination R-squared is more informative than SMAPE, MAE, MAPE, MSE and RMSE in regression analysis evaluation. PeerJ Computer Science, 7, 1-24. https://doi.org/10.7717/peerj-cs.623

Chiu, C.-A., Lu, M.-C., Zhong, Y.-L., Tsai, T.-Y., Liu, C.-J., & Ho, M.-C. (2023). Quantifying and Analyzing Brainwave Electroencephalography with Welch's Method. Sensors and Materials, 35(5), 1579-1586. https://doi.org/10.18494/SAM4065

de Looze, M. P., Bosch, T., Krause, F., Stadler, K. S., & O'Sullivan, L. W. (2016). Exoskeletons for industrial application and their potential effects on physical work load. Ergonomics, 59(5), 671-681. https://doi.org/10.1080/00140139.2015.1081988

Delorme, A., & Makeig, S. (2004). EEGLAB: an open source toolbox for analysis of single-trial EEG dynamics including independent component analysis. Journal of neuroscience methods, 134(1), 9-21. https://doi.org/10.1016/j.jneumeth.2003.10.009

Dimitrakopoulos, G. N., Kakkos, I., Dai, Z., Lim, J., deSouza, J. J., Bezerianos, A., & Sun, Y. (2017). Task-independent mental workload classification based upon common multiband EEG cortical connectivity. IEEE Transactions on Neural Systems and Rehabilitation Engineering, 25(11), 1940-1949. https://doi.org/10.1109/TNSRE.2017.2701002

Fan, J., & Smith, A. P. (2017). The Impact of Workload and Fatigue on Performance. Communications in Computer and Information Science, 726, 90-105. https://doi.org/10.1007/978-3-319-61061-0_6

Fox, S., Aranko, O., Heilala, J., & Vahala, P. (2019). Exoskeletons: Comprehensive, comparative and critical analyses of their potential to improve manufacturing performance. Journal of Manufacturing Technology Management, 31(6), 1261-1280. https://doi.org/10.1108/JMTM-01-2019-0023

Frølich, L., & Dowding, I. (2018). Removal of muscular artifacts in EEG signals: a comparison of linear decomposition methods. Brain informatics, 5(1), 13-22. https://doi.org/10.1007/s40708-017-0074-6

Gonsalves, N., Akanmu, A., Gao, X., Agee, P., & Shojaei, A. (2023). Industry Perception of the Suitability of Wearable Robot for Construction Work. Journal of Construction Engineering and Management, 149(5), 04023017. https://doi.org/10.1061/JCEMD4.COENG-12762

Gonsalves, N., Akanmu, A., Gao, X. H., Agee, P., & Shojaei, A. (2023). Industry Perception of the Suitability of Wearable Robot for Construction Work. Journal of Construction Engineering and Management, 149(5). https://doi.org/10.1061/JCEMD4.COENG-12762

Gonsalves, N. J., Ogunseiju, O. R., Akanmu, A. A., & Nnaji, C. A. (2021). Assessment of a passive wearable robot for reducing low back disorders during rebar work. Journal of Information Technology in Construction, 26, 936-952. https://doi.org/10.36680/j.itcon.2021.050

Gorgey, A. S. (2018). Robotic exoskeletons: The current pros and cons. World Journal of Orthopedics, 9(9), 112-119. https://doi.org/10.5312/wjo.v9.i9.112

Guo, H. L., Zhang, Z. T., Yu, R., Sun, Y. K., & Li, H. (2023). Action Recognition Based on 3D Skeleton and LSTM for the Monitoring of Construction Workers' Safety Harness Usage. Journal of Construction Engineering and Management, 149(4). https://doi.org/10.1061/JCEMD4.COENG-12542

Hamann, A., & Carstengerdes, N. (2022). Investigating mental workload-induced changes in cortical oxygenation and frontal theta activity during simulated flights. Scientific Reports, 12(1), 1-12. https://doi.org/10.1038/s41598-022-10044-y

Hernandez, C., Slaton, T., Balali, V., & Akhavian, R. (2019). A Deep Learning Framework for Construction Equipment Activity Analysis. Computing in Civil Engineering 2019: Data, Sensing, and Analytics, <Go to ISI>://WOS:000485219700061, 479-486.

Hodson, T. O. (2022). Root mean square error (RMSE) or mean absolute error (MAE): When to use them or not. Geoscientific Model Development Discussions, 15, 5481–5487. https://doi.org/10.5194/gmd-15-5481-2022

Hopstaken, J. F., Van Der Linden, D., Bakker, A. B., & Kompier, M. A. (2015). A multifaceted investigation of the link between mental fatigue and task disengagement. Psychophysiology, 52(3), 305-315. https://doi.org/10.1111/psyp.12339

Huang, J., Liu, Y., & Peng, X. (2022). Recognition of driver's mental workload based on physiological signals, a comparative study. Biomedical Signal Processing and Control, 71, 103094. https://doi.org/10.1016/j.bspc.2021.103094

Hwang, S., Jebelli, H., Choi, B., Choi, M., & Lee, S. (2018). Measuring workers' emotional state during construction tasks using wearable EEG. Journal of Construction Engineering and Management, 144(7), 04018050. https://doi.org/10.1061/(ASCE)CO.1943-7862.0001506

Iftikhar, M., Khan, S. A., & Hassan, A. (2018). A survey of deep learning and traditional approaches for EEG signal processing and classification. 2018 IEEE 9th annual information technology, electronics and mobile communication conference (IEMCON), https://doi.org/10.1109/IEMCON.2018.8614893

Itthipuripat, S., Wessel, J. R., & Aron, A. R. (2013). Frontal theta is a signature of successful working memory manipulation. Experimental brain research, 224, 255-262. https://doi.org/10.1007/s00221-012-3305-3

Jebelli, H., Hwang, S., & Lee, S. (2018a). EEG-based workers' stress recognition at construction sites. Automation in Construction, 93, 315-324. https://doi.org/10.1016/j.autcon.2018.05.027

Jebelli, H., Hwang, S., & Lee, S. (2018b). EEG signal-processing framework to obtain high-quality brain waves from an off-the-shelf wearable EEG device. Journal of computing in civil engineering, 32(1), 04017070. https://doi.org/10.1061/(ASCE)CP.1943-5487.0000719

Jenke, R., Peer, A., & Buss, M. (2014). Feature extraction and selection for emotion recognition from EEG. IEEE Transactions on Affective computing, 5(3), 327-339. https://doi.org/10.1109/TAFFC.2014.2339834

Käthner, I., Wriessnegger, S. C., Müller-Putz, G. R., Kübler, A., & Halder, S. (2014). Effects of mental workload and fatigue on the P300, alpha and theta band power during operation of an ERP (P300) brain–computer interface. Biological psychology, 102, 118-129. https://doi.org/10.1016/j.biopsycho.2014.07.014

Ke, J., Zhang, M., Luo, X., & Chen, J. (2021). Monitoring distraction of construction workers caused by noise using a wearable Electroencephalography (EEG) device. Automation in Construction, 125, 103598. https://doi.org/10.1016/j.autcon.2021.103598

Kim, S., Moore, A., Srinivasan, D., Akanmu, A., Barr, A., Harris-Adamson, C., Rempel, D. M., & Nussbaum, M. A. (2019). Potential of Exoskeleton Technologies to Enhance Safety, Health, and Performance in Construction: Industry Perspectives and Future Research Directions. Iise Transactions on Occupational Ergonomics & Human Factors, 7(3-4), 185-191. https://doi.org/10.1080/24725838.2018.1561557

Kingma, D. P., & Ba, J. (2014). Adam: A method for stochastic optimization. arXiv preprint arXiv:1412.6980, 10.48550/arXiv.1412.6980. https://doi.org/10.48550/arXiv.1412.6980

Koopman, A. S., Näf, M., Baltrusch, S. J., Kingma, I., Rodriguez-Guerrero, C., Babič, J., de Looze, M. P., & van Dieën, J. H. (2020). Biomechanical evaluation of a new passive back support exoskeleton. Journal of Biomechanics, 105, 109795. https://doi.org/10.1016/j.jbiomech.2020.109795

Kumar, N., & Kumar, J. (2016). Measurement of cognitive load in HCI systems using EEG power spectrum: an experimental study. Procedia Computer Science, 84, 70-78. https://doi.org/10.1016/j.procs.2016.04.068

Lee, H.-S., Kim, H., Park, M., Ai Lin Teo, E., & Lee, K.-P. (2012). Construction risk assessment using site influence factors. Journal of computing in civil engineering, 26(3), 319-330. https://doi.org/10.1061/(ASCE)CP.1943-5487.0000146

Liu, H., Lang, B., Liu, M., & Yan, H. (2019). CNN and RNN based payload classification methods for attack detection. Knowledge-Based Systems, 163, 332-341. https://doi.org/10.1016/j.knosys.2018.08.036

Liu, P. K., Chi, H. L., Li, X., & Li, D. S. (2020). Development of a Fatigue Detection and Early Warning System for Crane Operators: A Preliminary Study. Construction Research Congress 2020: Computer Applications, <Go to ISI>://WOS:000652190900012, 106-115.

Liu, Y., Li, X. L., Lai, J. R., Zhu, A. B., Zhang, X. D., Zheng, Z. M., Zhu, H. J., Shi, Y. Y., Wang, L., & Chen, Z. Y. (2021). The Effects of a Passive Exoskeleton on Human Thermal Responses in Temperate and Cold Environments. International Journal of Environmental Research and Public Health, 18(8). https://doi.org/10.3390/ijerph18083889

Longo, L. (2022). Modeling cognitive load as a self-supervised brain rate with electroencephalography and deep learning. Brain Sciences, 12(10), 1-22. https://doi.org/10.3390/brainsci12101416

Mantini, D., Franciotti, R., Romani, G. L., & Pizzella, V. (2008). Improving MEG source localizations: an automated method for complete artifact removal based on independent component analysis. NeuroImage, 40(1), 160-173. https://doi.org/10.1016/j.neuroimage.2007.11.022

Marchand, C., De Graaf, J. B., & Jarrasse, N. (2021). Measuring mental workload in assistive wearable devices: a review. Journal of Neuroengineering and Rehabilitation, 18(1), 1-15. https://doi.org/10.1186/s12984-021-00953-w

Massardi, S., Pinto-Fernandez, D., Babic, J., Dezman, M., Trost, A., Grosu, V., Lefeber, D., Rodriguez, C., Bessler, J., Schaake, L., Prange-Lasonder, G., Veneman, J. F., & Torricelli, D. (2023). Relevance of hazards in exoskeleton applications: a survey-based enquiry. Journal of Neuroengineering and Rehabilitation, 20(1), 1-13. https://doi.org/10.1186/s12984-023-01191-y

Mastropietro, A., Pirovano, I., Marciano, A., Porcelli, S., & Rizzo, G. (2023). Reliability of Mental Workload Index Assessed by EEG with Different Electrode Configurations and Signal Pre-Processing Pipelines. Sensors (Basel), 23(3), 1-14. https://doi.org/10.3390/s23031367

Mathew, A., Amudha, P., & Sivakumari, S. (2021). Deep learning techniques: an overview. Advanced Machine Learning Technologies and Applications: Proceedings of AMLTA 2020, 10.1007/978-981-15-3383-9_54, 599-608. https://doi.org/10.1007/978-981-15-3383-9_54

Missonnier, P., Deiber, M. P., Gold, G., Millet, P., Pun, M. G. F., Fazio-Costa, L., Giannakopoulos, P., & Ibanez, V. (2006). Frontal theta event-related synchronization: comparison of directed attention and working memory load effects. Journal of Neural Transmission, 113(10), 1477-1486. https://doi.org/10.1007/s00702-005-0443-9

Mitropoulos, P., & Memarian, B. (2013). Task demands in masonry work: Sources, performance implications, and management strategies. Journal of Construction Engineering and Management, 139(5), 581-590. https://doi.org/10.1061/(ASCE)CO.1943-7862.0000586

Miyamoto, K., Tanaka, H., & Nakamura, S. (2022). Online EEG-Based Emotion Prediction and Music Generation for Inducing Affective States. Ieice Transactions on Information and Systems, E105d(5), 1050-1063. https://doi.org/10.1587/transinf.2021EDP7171

Moon, T., Choi, H., Lee, H., & Song, I. (2015). Rnndrop: A novel dropout for rnns in asr. 2015 IEEE Workshop on Automatic Speech Recognition and Understanding (ASRU), https://doi.org/10.1109/ASRU.2015.7404775

Nussbaum, M. A., Lowe, B. D., de Looze, M., Harris-Adamson, C., & Smets, M. (2019). An Introduction to the Special Issue on Occupational Exoskeletons. Iise Transactions on Occupational Ergonomics & Human Factors, 7(3-4), 153-162. https://doi.org/10.1080/24725838.2019.1709695

Ogunseiju, O., Akinniyi, A., Gonsalves, N., Khalid, M., & Akanmu, A. (2023). Detecting Learning Stages within a Sensor-Based Mixed Reality Learning Environment Using Deep Learning. Journal of computing in civil engineering, 37(4). https://doi.org/10.1061/JCCEE5.CPENG-5169

Ogunseiju, O., Olayiwola, J., Akanmu, A., & Olatunji, O. A. (2022). Evaluation of postural-assist exoskeleton for manual material handling. Engineering Construction and Architectural Management, 29(3), 1358-1375. https://doi.org/10.1108/Ecam-07-2020-0491

Okunola, A., Akanmu, A. A., & Yusuf, A. O. (2023). Comparison of active and passive back-support exoskeletons for construction work: range of motion, discomfort, usability, exertion and cognitive load assessments. Smart and Sustainable Built Environment, Ahead-of-print(Ahead-of-print). https://doi.org/10.1108/SASBE-06-2023-0147

Persson, H. J., & Ståhl, G. (2020). Characterizing uncertainty in forest remote sensing studies. Remote Sensing, 12(3), 1-21. https://doi.org/10.3390/rs12030505

Picchiotti, M. T., Weston, E. B., Knapik, G. G., Dufour, J. S., & Marras, W. S. (2019). Impact of two postural assist exoskeletons on biomechanical loading of the lumbar spine. Applied ergonomics, 75, 1-7. https://doi.org/10.1016/j.apergo.2018.09.006

Poliero, T., Lazzaroni, M., Toxiri, S., Di Natali, C., Caldwell, D. G., & Ortiz, J. (2020). Applicability of an active back-support exoskeleton to carrying activities. Frontiers in Robotics and AI, 7, 579963. https://doi.org/10.3389/frobt.2020.579963

Pourmazaherian, M., Baqutayan, S. M. S., & Idrus, D. (2021). The role of the big five personality factors on accident: A case of accidents in construction industries. Journal of Science, Technology and Innovation Policy, 7(1), 34-43. https://doi.org/10.11113/jostip.v7n1.65

Qin, Y., & Bulbul, T. (2023a). An EEG-based mental workload evaluation for AR head-mounted display use in construction assembly tasks. Journal of Construction Engineering and Management, 149(9), 04023088. https://doi.org/10.1061/JCEMD4.COENG-13438

Qin, Y., & Bulbul, T. (2023b). Electroencephalogram-based mental workload prediction for using Augmented Reality head mounted display in construction assembly: A deep learning approach. Automation in Construction, 152, 104892. https://doi.org/10.1016/j.autcon.2023.104892

Qin, Y., Bulbul, T., & Withers, J. (2024). EEG-Based Classification of Cognitive Load and Task Conditions for AR Supported Construction Assembly: A Deep Learning Approach. In Computing in Civil Engineering 2023 (10.1061/9780784485231.030pp. 248-256). https://doi.org/10.1061/9780784485231.030

Raufi, B., & Longo, L. (2022). An Evaluation of the EEG alpha-to-theta and theta-to-alpha band Ratios as Indexes of Mental Workload. Frontiers in Neuroinformatics, 16, 1-16. https://doi.org/10.3389/fninf.2022.861967

Renaud, O., & Victoria-Feser, M.-P. (2010). A robust coefficient of determination for regression. Journal of Statistical Planning and Inference, 140(7), 1852-1862. https://doi.org/10.1016/j.jspi.2010.01.008

Ryu, K., & Myung, R. (2005). Evaluation of mental workload with a combined measure based on physiological indices during a dual task of tracking and mental arithmetic. International Journal of Industrial Ergonomics, 35(11), 991-1009. https://doi.org/10.1016/j.ergon.2005.04.005

Sauseng, P., Griesmayr, B., Freunberger, R., & Klimesch, W. (2010). Control mechanisms in working memory: a possible function of EEG theta oscillations. Neuroscience & Biobehavioral Reviews, 34(7), 1015-1022. https://doi.org/10.1016/j.neubiorev.2009.12.006

Scharinger, C., Kammerer, Y., & Gerjets, P. (2015). Pupil dilation and EEG alpha frequency band power reveal load on executive functions for link-selection processes during text reading. PloS one, 10(6), 1-24. https://doi.org/10.1371/journal.pone.0130608

Scharinger, C., Soutschek, A., Schubert, T., & Gerjets, P. (2015). When flanker meets the n-back: What EEG and pupil dilation data reveal about the interplay between the two central-executive working memory functions inhibition and updating. Psychophysiology, 52(10), 1293-1304. https://doi.org/10.1111/psyp.12500

Simon, M., Schmidt, E. A., Kincses, W. E., Fritzsche, M., Bruns, A., Aufmuth, C., Bogdan, M., Rosenstiel, W., & Schrauf, M. (2011). EEG alpha spindle measures as indicators of driver fatigue under real traffic conditions. Clinical Neurophysiology, 122(6), 1168-1178. https://doi.org/10.1016/j.clinph.2010.10.044

So, W. K., Wong, S. W., Mak, J. N., & Chan, R. H. (2017). An evaluation of mental workload with frontal EEG. PloS one, 12(4), 1-17. https://doi.org/10.1371/journal.pone.0174949

Spüler, M., Walter, C., Rosenstiel, W., Gerjets, P., Moeller, K., & Klein, E. (2016). EEG-based prediction of cognitive workload induced by arithmetic: a step towards online adaptation in numerical learning. Zdm Mathematics Education, 48, 267-278. https://doi.org/10.1007/s11858-015-0754-8

Srivastava, N., Hinton, G., Krizhevsky, A., Sutskever, I., & Salakhutdinov, R. (2014). Dropout: a simple way to prevent neural networks from overfitting. The journal of machine learning research, 15(1), 1929-1958. https://doi.org/10.5555/2627435.2670313

Staudemeyer, R. C., & Morris, E. R. (2019). Understanding LSTM--a tutorial into long short-term memory recurrent neural networks. arXiv preprint arXiv:1909.09586, 10.48550/arXiv.1909.09586, 1-42. https://doi.org/10.48550/arXiv.1909.09586

Teng, C., & Postle, B. R. (2021). Understanding occipital and parietal contributions to visual working memory: Commentary on Xu (2020). Visual cognition, 29(7), 401-408. https://doi.org/10.1080/13506285.2021.1883171

Vaidya, A. R., & Fellows, L. K. (2017). Chapter 22 - The Neuropsychology of Decision-Making: A View From the Frontal Lobes. In J.-C. Dreher & L. Tremblay (Eds.), Decision Neuroscience (10.1016/B978-0-12-805308-9.00022-1pp. 277-289). Academic Press. https://doi.org/10.1016/B978-0-12-805308-9.00022-1

Van Houdt, G., Mosquera, C., & Nápoles, G. (2020). A review on the long short-term memory model. Artificial Intelligence Review, 53, 5929-5955. https://doi.org/10.1007/s10462-020-09838-1

Varatharajah, Y., Chong, M. J., Saboo, K., Berry, B., Brinkmann, B., Worrell, G., & Iyer, R. (2017). EEG-GRAPH: a factor-graph-based model for capturing spatial, temporal, and observational relationships in electroencephalograms. Advances in neural information processing systems, 30, 5372-5381. https://openreview.net/pdf?id=rJVgWuZubr

Wang, D., Chen, J., Zhao, D., Dai, F., Zheng, C., & Wu, X. (2017). Monitoring workers' attention and vigilance in construction activities through a wireless and wearable electroencephalography system. Automation in Construction, 82, 122-137. https://doi.org/10.1016/j.autcon.2017.02.001

Wang, J., Ma, Y., Zhang, L., Gao, R. X., & Wu, D. (2018). Deep learning for smart manufacturing: Methods and applications. Journal of manufacturing systems, 48, 144-156. https://doi.org/10.1016/j.jmsy.2018.01.003

Wang, Y., Huang, Y., Gu, B., Cao, S., & Fang, D. (2023). Identifying mental fatigue of construction workers using EEG and deep learning. Automation in Construction, 151, 104887. https://doi.org/10.1016/j.autcon.2023.104887

Wei, W., Zha, S., Xia, Y., Gu, J., & Lin, X. (2020). A hip active assisted exoskeleton that assists the semi-squat lifting. Applied Sciences, 10(7), 2424. https://doi.org/10.3390/app10072424

Wu, L., Li, J., Wang, Y., Meng, Q., Qin, T., Chen, W., Zhang, M., & Liu, T.-Y. (2021). R-drop: Regularized dropout for neural networks. Advances in neural information processing systems, 34, 10890-10905. https://doi.org/10.48550/arXiv.2106.14448

Xi, X., Li, J., Wang, Z., Tian, H., & Yang, R. (2024). The effect of high-order interactions on the functional brain networks of boys with ADHD. The European Physical Journal Special Topics, 10.1140/epjs/s11734-024-01161-y, 1-13. https://doi.org/10.1140/epjs/s11734-024-01161-y

Yoo, G., Kim, H., & Hong, S. (2023). Prediction of Cognitive Load from Electroencephalography Signals Using Long Short-Term Memory Network. Bioengineering, 10(3), 1-15. https://doi.org/10.3390/bioengineering10030361

Young, M. S., Brookhuis, K. A., Wickens, C. D., & Hancock, P. A. (2015). State of Science: Mental Workload in Ergonomics. Ergonomics, 58, 1–17. https://doi.org/10.1080/00140139.2014.956151

Yusuf, A., Akanmu, A., Afolabi, A., & Murzi, H. (2023). Prediction of Cognitive Load during Industry-Academia Collaboration via a Web Platform 23rd International Conference on Construction Applications of Virtual Reality, Florence, Italy. https://library.oapen.org/bitstream/handle/20.500.12657/89150/1/9791221502893_06.pdf

Zarjam, P., Epps, J., & Lovell, N. H. (2015). Beyond subjective self-rating: EEG signal classification of cognitive workload. IEEE Transactions on Autonomous Mental Development, 7(4), 301-310. https://doi.org/10.1109/TAMD.2015.2441960

Zhang, H. (2022). A Mental Workload Evaluation Model Based on Improved Multibranch LSTM Network with Attention Mechanism. Advances in Multimedia, 2022, 1-11. https://doi.org/10.1155/2022/9601946

Zhang, R., Zong, Q., Dou, L., Zhao, X., Tang, Y., & Li, Z. (2021). Hybrid deep neural network using transfer learning for EEG motor imagery decoding. Biomedical Signal Processing and Control, 63, 102144. https://doi.org/10.1016/j.bspc.2020.102144

Zhao, R., Yan, R., Wang, J., & Mao, K. (2017). Learning to monitor machine health with convolutional bi-directional LSTM networks. Sensors, 17(2), 1-18. https://doi.org/10.3390/s17020273

Zhu, F., Kern, M., Fowkes, E., Afzal, T., Contreras-Vidal, J.-L., Francisco, G. E., & Chang, S.-H. (2021). Effects of an exoskeleton-assisted gait training on post-stroke lower-limb muscle coordination. Journal of Neural Engineering, 18(4), 046039. https://doi.org/10.1088/1741-2552/abf0d5